12-2016

Characterization of the recombination activities of the *Entamoeba histolytica* Rad51 recombinase

Andrew A. Kelso
Clemson University

Steven D. Goodson
Clemson University

Suchitra Chavan
Clemson University

Amanda F. Say
Clemson University

Audrey Turchick
Clemson University

See next page for additional authors

Authors
Andrew A. Kelso, Steven D. Goodson, Suchitra Chavan, Amanda F. Say, Audrey Turchick, Deepti Sharma, LeAnna L. Ledford, Erin Ratterman, Kristin Leskoske, Ada V. King, Christopher C. Attaway, Yura Bandera, Stephen H. Foulger, Alexander V. Mazin, Lesly A. Temesvari, and Michael G. Sehorn

HHS Public Access

Author manuscript

Mol Biochem Parasitol. Author manuscript; available in PMC 2017 November 01.

Published in final edited form as:

Mol Biochem Parasitol. 2016 ; 210(1-2): 71–84. doi:10.1016/j.molbiopara.2016.09.001.

Characterization of the recombination activities of the *Entamoeba histolytica* Rad51 recombinase

Andrew A. Kelso[a,b,1], **Steven D. Goodson**[a,b,1], **Suchitra Chavan**[b,c], **Amanda F. Say**[a], **Audrey Turchick**[a], **Deepti Sharma**[a], **LeAnna L. Ledford**[a], **Erin Ratterman**[a], **Kristin Leskoske**[a], **Ada V. King**[c], **Christopher C. Attaway**[c], **Yura Bandera**[d,e], **Stephen H. Foulger**[d,e], **Alexander V. Mazin**[f], **Lesly A. Temesvari**[b,c,g], and **Michael G. Sehorn**[a,d,g,*]

[a]Department of Genetics and Biochemistry, Clemson University, Clemson, SC 29634, USA

[b]Eukaryotic Pathogens Innovation Center, Clemson University, Clemson, SC 29634, USA

[c]Department of Biological Sciences, Clemson University, Clemson, SC 29634, USA

[d]Center for Optical Materials Science and Engineering Technologies, Clemson University, Clemson, SC 29634, USA

[e]Department of Material Science and Engineering, Clemson University, Clemson, SC 29634, USA

[f]Department of Biochemistry and Molecular Biology, Drexel University College of Medicine, Philadelphia, PA 19102, USA

[g]Clemson University School of Health Research, Clemson, SC 29634, USA

Abstract

The protozoan parasite responsible for human amoebiasis is *Entamoeba histolytica*. An important facet of the life cycle of *E. histolytica* involves the conversion of the mature trophozoite to a cyst. This transition is thought to involve homologous recombination (HR), which is dependent upon the Rad51 recombinase. Here, a biochemical characterization of highly purified *eh*Rad51 protein is presented. The *eh*Rad51 protein preferentially binds ssDNA, forms a presynaptic filament and possesses ATP hydrolysis activity that is stimulated by the presence of DNA. Evidence is provided that *eh*Rad51 catalyzes robust DNA strand exchange over at least 5.4 kilobase pairs. Although the homologous DNA pairing activity of *eh*Rad51 is weak, it is strongly enhanced by the presence of two HR accessory cofactors, calcium and Hop2-Mnd1. The biochemical system described herein was used to demonstrate the potential for targeting *eh*Rad51 with two small molecule inhibitors of human RAD51. We show that 4,4′-diisothiocyanostilbene-2,2′-disulfonic acid (DIDS) inhibited *eh*Rad51 by interfering with DNA binding and attenuated encystation in *Entamoeba invadens,* while B02 had no effect on *eh*Rad51 strand exchange activity. These results provide insight into the underlying mechanism of homology-directed DNA repair in *E. histolytica.*

[*]Corresponding author at: Department of Genetics and Biochemistry, Clemson University, Clemson, SC 29634, USA., msehorn@clemson.edu (M.G. Sehorn).

[1]These authors contributed equally.

Keywords

Homologous recombination; *Entamoeba histolytica*; RAD51; DNA repair; Recombinase inhibitors

1. Introduction

Homologous recombination (HR) is a critical pathway involved in the repair of chromosomes with deleterious DNA double-strand breaks (DSBs) and interstrand crosslinks that may occur upon exposure to chemical reagents and ionizing radiation. HR is also important for the repair of blocked or stalled replication forks and is crucial for the proper segregation of homologous chromosomes in Meiosis I [1–7]. When the cell encounters a DSB, the ends of the break are nucleolytically processed to yield 3′ single-strand DNA (ssDNA) overhangs. The exposed 3′ overhang serves as the nucleation site for a DNA recombinase to form a nucleoprotein filament known as the presynaptic filament, which is responsible for the homology search in the sister chromatid. Once homology is found, the nucleoprotein filament invades the homologous duplex DNA resulting in the displacement of the homologous strand to form a displacement loop (D-loop). Following the formation of a D-loop, the recombinase facilitates strand exchange [8], and the invading strand primes DNA synthesis to restore the damaged DNA. In most eukaryotes, there are two orthologs of the *Escherichia coli* RecA recombinase, Rad51 and Dmc1, which are responsible for the homology search and strand exchange of HR [9]. Dmc1 is a meiosis-specific recombinase, and Rad51 is ubiquitously expressed, yet plays a supporting role in meiosis [10]. The activities of the recombinases during HR are regulated by a variety of different accessory cofactors, including replication protein A (RPA) [11], calcium [12–16], and Hop2-Mnd1 [1,13,17–20].

Entamoeba histolytica is a protozoan parasite responsible for amoebic dysentery and amoebic liver abscess. Potential hosts are most commonly exposed to *E. histolytica* through contaminated food and water sources, which puts 50 million humans at risk for amebic dysentery and liver abscesses yearly, with approximately 70,000 deaths worldwide [21–23]. The life cycle of *E. histolytica* involves host ingestion of tetra-nucleated cysts that undergo several divisions to produce eight trophic amoebae through a process known as excystation. The mature trophozoite (containing a single nucleus) can colonize the colon [24], where it divides by binary fission and feeds on bacteria, host cells, and host cell debris. As a result of unknown cues, the pathogen completes the life cycle by duplicating its genome and forming tetra-nucleated, environmentally-stable cysts in a process known as encystation. This process facilitates host-to-host spread. It is unknown if there is genetic exchange among the four nuclei in the *E. histolytica* cyst; however, *Giardia intestinalis*, another cyst-forming enteric pathogen, possesses two nuclei that may exchange genetic information [25]. It is conceivable that the ability of *E. histolytica* to go through diverse life stages, including genome duplications and spontaneous genome amplification, is likely mediated through HR [26–28]. In support of this argument, the *E. histolytica* genome contains genes homologous to the majority of the RAD52 epistasis group of genes [29–31]. The RAD52 epistasis group of genes accounts for the core DNA repair genes of HR (*RAD50, RAD51, RAD52, RAD54, RAD55, RAD57, RAD59, RDH54*, *MRE11*, and *XRS2*), which are highly conserved among

eukaryotes [32]. In recent years, *E. histolytica* was shown to differentially express this group of genes in response to DNA damage [29,30], and HR was demonstrated *in vivo* [33]. Other protozoan parasites are reported to utilize HR as a means for adaptation and survival in host environments. *Trypanosoma brucei* employs the Rad51 recombinase to recombine variant surface glycoproteins to evade the host immune response. Specifically, *T. brucei* parasites that contain defective Rad51 show a decreased ability to undergo variant surface glycoproteins switching [34]. *Leishmania major* use HR to amplify antibiotic resistance genes and up-regulate the expression of Rad51 in response to DNA damage [35]. The role of the Rad51 recombinase in *E. histolytica* (*eh*Rad51) is largely unknown. In this study, we purified recombinant *eh*Rad51 and biochemically characterized its recombinase activities. Our results will be valuable for defining the mechanism of *eh*Rad51-mediated recombination in *E. histolytica*.

2. Materials and methods

2.1. DNA substrates and small molecules

All oligonucleotides were purchased from Integrated DNA Technologies, and the sequences can be found in Table 1. H3 was used as ssDNA in the DNA binding assay. H3c was annealed to H3 for dsDNA in the DNA binding assay. OL83-1 (ssDNA) and the complex OL83-1/OL83-2 (dsDNA) were used in the oligonucleotide strand exchange assay. OL90 (ssDNA) was used in the nuclease protection assay and D-loop assay. All oligonucleotides indicated as radiolabeled were done so using T4 polynucleotide kinase and [^{32}P-γ]-ATP as described [15]. ϕX174 (+) virion ssDNA and ϕX174 replicative form I dsDNA were purchased from New England BioLabs; the ϕX174 replicative form I dsDNA was linearized with *Apa*LI (New England BioLabs). pBluescript was purified from *E. coli* using a Plasmid Giga kit (Qiagen). 4,4′-diisothiocyanostilbene-2,2′-disulfonic acid, DIDS was purchased from Sigma-Aldrich. (*E*)-2-(2-(pyridin-3-yl)vinyl)quinazolin-4(3H)-one, B02 was purchased from Ryan Scientific Inc. [36].

2.2. Isolation and modification of the gene encoding *E. histolytica* Rad51

The isolation and modification of the *E. histolytica* Rad51 gene (XM 648984) to create the pET-*ehRAD51*-(HIS)$_6$ bacterial expression plasmid was previously described [37].

2.3. Growth of *E. invadens*

E. invadens (strain IP-1) (1–2 × 10^6 cells/ml) were seeded into LYI-S-2 [38] axenic medium in 15 ml glass screw cap tubes at 25 °C in the absence or presence of DIDS (30 μM or 150 μM). After 48 h, cell viability was assessed by hemocytometer-based cell counting with Trypan blue exclusion.

2.4. Encystation of *E. invadens*

To induce encystation, *E. invadens* trophozoites (5 × 10^6) were transferred to encystation medium, LYI-LG [39], in the absence or presence of DIDS (30 μM or 150 μM). After 48 h, encystation efficiency was estimated by incubation in 0.1% (v/v) sarkosyl in PBS on ice for 40 min, which lyses trophozoites. This allowed the percentage of mature detergent-resistant cysts in a population to be calculated.

2.5. Expression and purification of *eh*Rad51

The purification of *eh*Rad51 was performed as previously described [37] with modifications. Briefly, *eh*Rad51 was expressed in the BL21 (Novagen) strain of *E. coli* cells. The cells were grown at 37 °C until an OD_{600} = 1.0 and induced with 0.4 mM IPTG at 16 °C for 20 h. The cells were harvested by centrifugation. All successive steps in the purification were performed at 4 °C. The cell paste (40 g) was resuspended in Buffer A (50 mM Tris-HCl pH 7.5, 1 mM EDTA, 10% sucrose, 250 mM KCl, 1 mM 2-mercaptoethanol, 0.01% Igepal, 0.1 mg/ml lysozyme, 5 mM benzamide, 1 mM PMSF, and a combination of protease inhibitors at 5 μg/ml: aprotinin, chymostatin, leupeptin, and pepstatin A) followed by sonication. The lysate was clarified using ultracentrifugation at 100,000 x *g* (Beckman Ti-45 rotor) for 90 min. The clarified lysate was incubated with 3 ml of Ni-NTA Sepharose (GE Healthcare) overnight. The lysate containing the Ni-NTA matrix was poured into a glass column with an internal diameter of 1 cm (BioRad). After a wash with Buffer B (20 mM KH_2PO_4 pH 7.5, 10% glycerol, 1 mM EDTA) containing 150 mM KCl, the bound protein was eluted from the Ni-NTA beads in Buffer B containing 150 mM KCl and 500 mM imidazole. The eluate containing *eh*Rad51 was loaded onto an 8 ml hydroxyapatite column (BioRad) equilibrated with Buffer B containing 100 mM KCl. The column was developed using a linear gradient of Buffer B containing 0–300 mM KH_2PO_4. The peak fractions containing *eh*Rad51 were pooled and loaded onto a 2 ml Source 15Q column (GE Healthcare) equilibrated with Buffer B containing 100 mM KCl. The column was developed using a linear gradient of Buffer B containing 100–450 mM KCl. The fractions containing *eh*Rad51 were pooled, concentrated to 8 mg/ml, and frozen in aliquots at −80 °C. The yield was 12 mg of purified *eh*Rad51.

2.6. Expression and purification of other proteins

Existing protocols were used to express and purify *E. histolytica* Dmc1 (*eh*Dmc1) [37], murine Hop2-Mnd1 [40], human RAD51, and human RPA [41].

2.7. ATP hydrolysis

*eh*Rad51 (10 μM) was incubated with 1.5 mM [^{32}P-γ]-ATP in Buffer C (25 mM Tris-HCl pH 7.5, 0.1 mg/ml BSA, 1 mM DTT, 2.4 mM $MgCl_2$, 20 mM KCl) in the absence or presence of ϕX174 (+) virion ssDNA (90 μM nucleotides) or linearized ϕX174 replicative form I dsDNA (90 μM base pairs) at 37 °C. At the indicated times, the reactions were stopped by the addition of an equal volume of 0.5 mM EDTA and subjected to thin-layer chromatography using polyethyleneimine-cellulose plates (Sigma Aldrich). The amount of ATP hydrolysis was determined using a phosphorimager (Typhoon FLA 7000, GE Healthcare). When testing the effects of DIDS on ATP hydrolysis activity, 67 μM of DIDS was incubated with *eh*Rad51 in the absence or presence of ϕX174 ssDNA or ϕX174 dsDNA. The reactions were stopped at the indicated times and treated as described above.

2.8. DNA binding

Increasing concentrations of *eh*Rad51 (as indicated) were incubated in Buffer D (25 mM Tris-HCl pH 7.4, 0.1 mg/ml BSA, 1 mM DTT, 2.4 mM $MgCl_2$, 2 mM ATP) in the presence of 32P-radiolabeled H3 (ssDNA) or ^{32}P-radiolabeled H3/H3c (dsDNA) for 20 min at 37 °C. Reaction products were subjected to 12% non-denaturing gel electrophoresis. The gels were

dried on Whatman cellulose chromatography paper (Sigma-Aldrich), and analyzed using a phosphorimager (GE Healthcare Life Sciences Typhoon FLA 7000). When testing the effect of DIDS on ssDNA binding, *eh*Rad51 (7 μM) was incubated with ^{32}P-radiolabeled H3 (ssDNA) in the presence of increasing amounts of DIDS (5, 10, 15, 20, 30, and 40 μM). Also, increasing concentrations of DIDS (20, 40, 80, 100, 150, and 200 μM) were incubated with *eh*Rad51 (35 μM) in the presence of ^{32}P-radiolabeled H3/H3c (dsDNA). The reactions products were processed and analyzed as described above.

2.9. Nuclease protection assay

To determine the ability of *eh*Rad51 to form a stable nucleoprotein filament, *eh*Rad51 (2.5 μM) was incubated with ^{32}P-radiolabeled OL90 (3 μM nucleotides) at 37 °C in Buffer C containing 2 mM ATP for 1, 2.5, 5, 7.5, and 10 min (as indicated) at which point DNase I (2 units; Promega) was added to the reaction. The reaction was incubated for 15 min, and the reaction products were deproteinized with the addition of SDS (0.5%) and Proteinase K (1.5 μg/ml). The products were separated using 12% native polyacrylamide gel electrophoresis. The gels were dried on Whatman cellulose chromatography paper (Sigma-Aldrich), and analyzed using a phosphorimager (GE Healthcare Life Sciences Typhoon FLA 7000). When testing the nucleotide dependence of filament stability, *eh*Rad51 (2.5 μM) was incubated with ^{32}P-radiolabeled OL90 (3 μM nucleotides) at 37 °C in Buffer C that was nucleotide free or contained ATP, ADP, ATP-γ-S or AMP-PNP (2 mM) for 10 min at which point DNase I was added to the reaction. The reactions were processed and analyzed as described above. When testing the filament stability in the presence of DIDS, we used the same amount of DNA and *eh*Rad51 used in the DNA binding. Here, *eh*Rad51 (7 μM) incubated with increasing concentrations of DIDS (5, 10, 15, 20, 30, and 40 μM). The reactions were processed and analyzed as previously described.

2.10. Strand exchange with plasmid-length DNA substrates

Increasing concentrations of *eh*Rad51 (4, 6, 8, 10, 12, 14, and 16 μM) were incubated with ϕX174 virion ssDNA (30 μM nucleotides) in Buffer D containing 16 mM creatine phosphate and 36 μg/ml creatine kinase at 37 °C. After a 10 min incubation, RPA (3.8 μM) and 150 mM KCl were added to the reactions, followed by an additional 8 min incubation at 37 °C. Addition of linearized double-stranded ϕX174 DNA (30 μM base pairs) and spermidine (4 mM) initiated the reaction. The reactions were deproteinized after 90 min by the addition of SDS (0.5%) and Proteinase K (0.5 μg/ml). The reaction products were separated on a 0.9% agarose gel, stained with ethidium bromide, and visualized using Image Lab software (BioRad).

2.11. Oligonucleotide-based strand exchange

Increasing concentrations of *eh*Rad51 (0.25, 0.5, 0.75, and 1 μM) were incubated with unlabeled OL83-1 (3 μM nucleotides) in Buffer C containing 2 mM ATP for 10 min at 37 °C. Duplex DNA (^{32}P-radiolabeled OL83-1/OL83-2; 3 μM base pairs) and spermidine (4 mM) were added to the reactions followed by a 60 min incubation at 37 °C before being deproteinized with the addition of SDS (0.5%) and Proteinase K (0.5 μg/ml). When testing the nucleotide dependence, *eh*Rad51 (1 μM) was incubated with unlabeled OL83-1 (3 μM nucleotides) in Buffer C containing either no nucleotide, ATP, ADP, ATP-γ-S, or AMP-PNP

(all at 2 mM) for 10 min at 37 °C. The reactions were deproteinized as described above, and the reaction products were separated using 10% native polyacrylamide gel electrophoresis and analyzed using a phosphorimager (GE Healthcare Life Sciences Typhoon FLA 7000). To test the stimulatory effect of calcium or mHop2-Mnd1 on *eh*Rad51 DNA strand exchange activity, a time course analysis was performed. The experiment was processed in the same manner as above, except for the incubation of *eh*Rad51 (1 μM) in the absence or presence of $CaCl_2$ (2 mM), mHop2-Mnd1 (0.6 μM; H2M1), or both $CaCl_2$ and mHop2-Mnd1. After the addition of duplex DNA and spermidine, the reaction products were deproteinized after 2.5, 5, 7.5, 10, 12.5, 15, 30, 45, and 60 min. The reaction products were separated on 12% polyacrylamide gels and analyzed using a phosphorimager. When testing *eh*Rad51 strand exchange activity in the presence of DIDS, *eh*Rad51 (1 μM) was incubated with increasing concentrations of DIDS (2.5, 5, 10, 15, 20, 30, and 40 μM) under the experimental conditions described above. The reaction products were analyzed as described above. When testing B02, the reactions were processed similar to a previous report [36]. Briefly, human RAD51 (1 μM), *eh*Rad51 (1 μM), or *eh*Dmc1 (1 μM) was incubated with OL83-1 in Buffer C containing ATP (2 mM) and $CaCl_2$ (1 mM). Increasing concentrations (100, 200, and 300 μM) of B02 (diluted in DMSO—reactions contained 6% DMSO final concentration) were added to the reactions and incubated for 20 min before the addition of duplex DNA and spermidine. An additional lane of human RAD51 was tested in the absence of DMSO under the same reaction conditions. The reactions incubated for 60 min before deproteinization. The reaction products were resolved and analyzed as described above.

2.12. mHop2-Mnd1 pull-downs

To determine the interaction of *eh*Rad51 with mHop2-Mnd1, a pull-down was performed as described [37]. Briefly, mHop2-Mnd1 (3.5 mg) and BSA (5 mg) were immobilized on 0.5 ml of Affi-gel 15 matrix (BioRad), separately, according to the manufacturer's instructions. *eh*Rad51 (7 μg) was incubated with 17.5 μl of Affi-mHop2-Mnd1 or Affi-BSA in Buffer B containing 100 mM KCl at 4 °C with agitation. After a 60 min incubation at 4 °C, the supernatant was removed, and the beads were washed three times with Buffer B containing 100 mM KCl. An equal volume of SDS loading dye (160 mM Tris-HCl pH 6.8, 60% glycerol, 4% SDS (w/v)) was added to each sample, and an aliquot of the supernatant, wash, and eluate were separated using 12% SDS-PAGE. The gel was stained with Coomassie blue.

2.13. D-loop assay

*eh*Rad51 (2 μM) was incubated with the ^{32}P-radiolabeled OL90 (4.5 μM) in Buffer D containing 16 mM creatine phosphate and 36 μg/ml creatine kinase for 5 min at 37 °C. $CaCl_2$ (0.5 mM) was added to the reaction (where indicated) followed by a 5 min incubation at 37 °C. This was followed by the addition of mHop2-Mnd1 (0.16 μM; H2M1), where indicated, and another 5 min incubation at 37 °C. The reactions were then initiated by the addition of pBlue-script (35 μM base pairs). At 0.5, 1, 2, 6, and 14 min the reactions were deproteinized with the addition of SDS (0.5%) and Proteinase K (0.5 μg/ml). Reaction products were resolved using 0.9% agarose gel electrophoresis, dried on DE81 anion exchange paper (GE Healthcare), and analyzed using a phosphorimager (GE Healthcare Life Sciences Typhoon FLA 7000).

2.14. Statistical analysis

The *in vitro* assays each had a minimum of three separate experiments, and error bars for each graph represent SEM. The effect of DIDS on viability and encystation of *E. invadens* was carried out as three biological replicates. All values are given as means ± SD. Statistical analyses were performed using GraphPad Prism Version 6.05. Comparisons of two groups were carried out using an unpaired two-tailed T-test. *P* values less than 0.05 were considered statistically significant.

3. Results

3.1. Isolation and purification of *eh*Rad51

E. histolytica was reported to overexpress *eh*Rad51 in response to DNA damage [29] suggesting that *eh*Rad51 was a functional recombinase. Lopez-Casamichana et al. (2008) provided evidence that partially purified recombinant *eh*Rad51 bound DNA and was capable of homologous DNA pairing to form a D-loop [29]. While these studies were important to show that *eh*Rad51 was indeed a functional recombinase, the lack of biochemical characterization is an impediment to understanding its role in HR in *E. histolytica*. Here, we sought to provide a thorough biochemical examination of *eh*Rad51 and its activities. We first cloned the *RAD51* gene from the *E. histolytica* genome. The sequence encoding the 6 histidine epitope tag was fused to the 5′ end of the *ehRAD51* gene by PCR and was inserted into a bacterial expression plasmid to be used for protein production [37]. Using a combination of affinity and ion exchange chromatography, *eh*Rad51 was purified to near homogeneity (Fig. 1A).

3.2. ATP hydrolysis by *eh*Rad51 is stimulated by the presence of DNA

Analysis of the primary sequence of the *RAD51* gene from *E. histolytica* revealed the presence of the conserved Walker A and B motifs (Fig. 1 in [42]) known to be important for binding and hydrolysis of ATP. To determine if *eh*Rad51 possessed the ability to hydrolyze ATP, purified *eh*Rad51 was incubated with saturating amounts of [^{32}P-γ]-ATP. The reaction products were resolved using thin-layer chromatography, and the results from three independent experiments indicated relatively weak hydrolysis (7%; Fig. 1B). Previous reports indicated the presence of DNA stimulated the ATP hydrolysis activity of human and yeast Rad51 [43,44]. To determine if DNA stimulated the ATPase activity of *eh*Rad51, we incubated *eh*Rad51 with saturating amounts of ϕX174 (+) virion ssDNA or linearized ϕX174 replicative form I dsDNA and [^{32}P-γ]-ATP. Our results show that DNA stimulated the ATP hydrolysis activity of *eh*Rad51 (Fig. 1B). The greatest stimulation occurred in the presence of ssDNA (32%) while a modest stimulation of ATP hydrolysis (17%) occurred in the presence of dsDNA (Fig. 1B). These results are in agreement with those reported for Rad51 proteins from other organisms [43–47].

3.3. *eh*Rad51 binds DNA

The stimulation of the ATP hydrolysis activity of *eh*Rad51 by the presence of ssDNA or dsDNA suggested *eh*Rad51 might bind DNA. To address this notion, an electrophoretic mobility shift assay (EMSA) was performed. In this assay, increasing concentrations of

*eh*Rad51 were incubated with ^{32}P-labeled ssDNA or dsDNA. The reaction products were resolved using non-denaturing polyacrylamide gel electrophoresis. Our results show that *eh*Rad51 binds both ssDNA and dsDNA in concentration-dependent manner (Fig. 1C and 1D, respectively). The *eh*Rad51-DNA complexes migrated with reduced mobility through the acrylamide gel. At sub-saturating concentrations, *eh*Rad51 appeared to display cooperative binding. *Eh*Rad51 showed a preference for ssDNA over dsDNA as 5-fold more *eh*Rad51 was required to reach saturation than for ssDNA (Fig. 1C and 1D, respectively). Our results show that *eh*Rad51 bound both ssDNA and dsDNA with a strong preference for ssDNA.

3.4. *eh*Rad51 forms a presynaptic filament

RecA and its eukaryotic orthologs, Rad51 and Dmc1, form right-handed helical filaments on ssDNA in the presence of ATP [13,47–51]. To test the formation of a presynaptic filament, we utilized a nuclease protection assay [15,37,45,52]. In this assay, *eh*Rad51 is incubated with ^{32}P-labeled ssDNA in the presence of ATP to allow for filament formation, followed by the addition of DNase I to degrade any exposed DNA. If *eh*Rad51 forms a filament, there will be protection of the ^{32}P-labeled ssDNA from DNase I. As shown in Fig. 2A, *eh*Rad51 forms a stable nucleoprotein filament within one minute and maintains protection of the ^{32}P-labeled ssDNA during the course of the experiment (Fig. 2A, lanes 3–7) in the presence of ATP. To determine what nucleotides facilitated presynaptic filament formation by *eh*Rad51, we performed the nuclease protection assay as described above with the exception that ATP was substituted with the slowly hydrolyzable ATP analog, ATP-γ-S; the non-hydrolyzable ATP analog, AMP-PNP; or ADP. Our results show that *eh*Rad51 formed a stable presynaptic filament in the presence of ATP and AMP-PNP (Fig. 2B, lanes 3 and 6). The integrity of the filament was slightly compromised in the presence of ATP-γ-S (Fig. 2B, lane 5). Surprisingly, in the presence of ADP, *eh*Rad51 was quite adept at forming a presynaptic filament that protected the ^{32}P-labeled ssDNA (Fig. 2B, lane 7). The absence of nucleotide did not support filament formation by *eh*Rad51 (Fig. 2B, lane 4). Taken together, these data suggest that formation of a stable *eh*Rad51 presynaptic filament is dependent upon binding a nucleotide but not its hydrolysis.

3.5. *eh*Rad51 mediates plasmid length DNA strand exchange

The capability of *eh*Rad51 to form a presynaptic filament led us to ask if *eh*Rad51 possessed the ability to promote DNA strand exchange. To address this question, we used a three-strand assay that utilizes ϕX174 DNA viral (+) ssDNA and linearized ϕX174 dsDNA that is 5.4 kilobase pairs in length to monitor DNA strand exchange [37,44,48]. In this assay, *eh*Rad51 was incubated with circular ϕX174 ssDNA to allow for filament formation followed by the addition of RPA. RPA is a ssDNA binding protein that prevents the formation of secondary structure in ssDNA. The DNA strand exchange reaction is initiated by the addition of linearized ϕX174 dsDNA. Early in strand exchange, a joint-molecule forms. The joint-molecule is extended by *eh*Rad51, displacing the homologous linear ssDNA to produce a nicked-circular molecule (Fig. 3A). In a concentration dependent manner, *eh*Rad51 catalyzed the formation of joint-molecules (Fig. 3B, lane 2) that were extended by DNA strand exchange to yield a nicked-circular dsDNA product (Fig. 3B, lanes 3–8). The optimal DNA strand exchange activity occurred at 10 μM *eh*Rad51 (Fig. 3B, lane

5 and Fig. 3C). This corresponds to the expected molar ratio of three nucleotides per monomer of *eh*Rad51 protein that was reported for human and *Saccharomyces cerevisiae* Rad51 [44,51,53]. These findings demonstrate that *eh*Rad51 catalyzed robust DNA strand exchange over thousands of base pairs.

3.6. *eh*Rad51 catalyzes nucleotide-dependent DNA strand exchange

The ability of Rad51 to catalyze DNA strand exchange is dependent upon the ability to bind, but not hydrolyze ATP in many species [43,45,54–56]. Since *eh*Rad51 formed a presynaptic filament in the presence of ATP, AMP-PNP, ATP-γ-S, and ADP, we wished to determine if *eh*Rad51 required ATP binding or hydrolysis to catalyze DNA strand exchange using an oligonucleotide DNA strand exchange system. In this assay, *eh*Rad51 was incubated with an unlabeled ssDNA oligonucleotide to allow filament formation. The reaction was initiated by the addition of radiolabeled duplex DNA, where the ^{32}P-radiolabeled strand of the duplex DNA is homologous to the unlabeled ssDNA located within the *eh*Rad51-ssDNA filament. If *eh*Rad51 promotes DNA strand exchange, the ^{32}P-oligonucleotide will be displaced from the dsDNA complex and exchanged for the unlabeled strand within the *eh*Rad51 filament (Fig. 4A). We found that *eh*Rad51 catalyzed DNA strand exchange in the presence of ATP in a concentration dependent manner (Fig. 4B, lanes 2–5). In the absence of a nucleotide, DNA strand exchange was not observed (Fig. 4B, lane 6). When AMP-PNP was substituted for ATP, there was only a slight reduction (4%) in the amount of product formed (Fig. 4B, compare lane 8 to 5). Substitution of ATP with ATP-γ-S or ADP failed to support *eh*Rad51-mediated DNA strand exchange (Fig. 4B, lanes 7 and 9). These results indicate that *eh*Rad51 facilitates DNA strand exchange that is dependent on nucleotide binding and not its hydrolysis.

3.7. *eh*Rad51 promotes weak D-loop formation

The fact that *eh*Rad51 can form a stable presynaptic filament that invades duplex DNA to promote DNA strand exchange suggests that it should be able to catalyze the formation of D-loops through homologous DNA pairing. To confirm this idea, a D-loop formation assay was performed [15,37,48]. In this assay, *eh*Rad51 was incubated with a ^{32}P-radiolabeled ssDNA oligonucleotide to form a presynaptic filament. The ssDNA oligonucleotide is homologous to a region within the supercoiled pBluescript dsDNA plasmid. Upon addition of the dsDNA plasmid, the *eh*Rad51 presynaptic filament searches for homology between the radiolabeled ssDNA and the dsDNA. Once homology is located, the presynaptic filament invades the duplex DNA, displacing the homologous strand to produce a D-loop (Fig. 5A). Using this assay, a time course analysis was performed which revealed *eh*Rad51 weakly forms D-loop (0.5%, Fig. 5B, lanes 2–6). The weak D-loop forming activity of *eh*Rad51 seen using our D-loop formation assay resembles the relatively low level of D-loop formation activity reported for human RAD51 [13]. In the same report, the presence of calcium enhanced the D-loop formation of human RAD51 [13]. Guided by this study, we examined the effect of calcium on *eh*Rad51 D-loop formation. Our results show that calcium increased the D-loop forming activity of *eh*Rad51 4-fold (2%; Fig. 5B, lanes 8–12).

3.8. *eh*Rad51 interacts with mHop2-Mnd1

HR accessory factors are known to modulate the activity of the Rad51 and Dmc1 recombinases [6]. One of these accessory factors, HOP2-MND1, interacts with and greatly enhances the D-loop formation activity of the human RAD51 and DMC1 recombinases [57,58]. Petukhova et al. (2005) [40] showed that murine Hop2-Mnd1 could physically interact with both human RAD51 and DMC1 and stimulate their D-loop formation activity. This is likely due to the high degree of homology between the human and murine RAD51 (99% identity) and DMC1 (97% identity) recombinases (Fig. 2 in [42]). *E. histolytica* has the *HOP2* and *MND1* genes and their expression is upregulated during encystation in *E. histolytica* at the same time as *eh*Rad51 and *eh*Dmc1 [33]. Based on these studies, we wanted to determine if *eh*Hop2-Mnd1 would interact with *eh*Rad51 to promote the D-loop formation activity of *eh*Rad51. Unfortunately, purified *eh*Hop2-Mnd1 protein complex is not currently available. Notably, most of what is known about Hop2-Mnd1 is derived from studies using murine Hop2-Mnd1 (mHop2-Mnd1) with human RAD51 and DMC1 [17,20,40,59]. In addition to these studies, Ploquin et al. (2007) showed mHop2-Mnd1 interacted with *Schizosaccharomyces pombe* Rad51 (*Sp*Rad51) [19] despite lower sequence identity (74%) between *Sp*Rad51 and murine Rad51 (Fig. 2 in [42]). The ability of mHop2-Mnd1 to interact with human RAD51, human DMC1, *Sp*Rad51, and *eh*Dmc1 [17,19,37,40,60] combined with the sequence identity of *eh*Rad51 with murine RAD51 (65% identity) that is close to that of *Sp*Rad51 and murine RAD51 (74% identity) (Fig. 2 in [42]), led us to reason that mHop2-Mnd1 may interact with *eh*Rad51 thereby potentially enhancing its recombination activities. We first determined if mHop2-Mnd1 interacted with *eh*Rad51 by performing an affinity pull-down assay using either bovine serum albumin (BSA) or purified mHop2-Mnd1 immobilized on Affi-gel matrix [37]. In this reaction, *eh*Rad51 was incubated with Affi-mHop2-Mnd1 beads. The beads were extensively washed to remove non-specifically bound proteins. The remaining proteins bound to the Affi-mHop2-Mnd1 beads were eluted. As shown in Fig. 6A, *eh*Rad51 was located in the elution fraction, indicating a physical interaction with mHop2-Mnd1 (Fig. 6A, lanes 2–4). When *eh*Rad51 was incubated with Affi-BSA, *eh*Rad51 was located in the supernatant, indicating there was no physical interaction with BSA or non-specific interaction of *eh*Rad51 with the Affi-gel matrix (Fig. 6A, lanes 5–7). Our findings indicate mHop2-Mnd1 interacts specifically with *eh*Rad51. The sequence homology between the human and *E. histolytica* recombinases is 66% for Rad51 and 61% for Dmc1, and the conservation between human and *E. histolytica* Hop2 and Mnd1 is 31% and 43%, respectively. The interaction between mHop2-Mnd1 and both *E. histolytica* recombinases [37] illustrates the evolutionary importance of the interaction between Hop2-Mnd1 and Rad51.

3.9. mHop2-Mnd1 stimulates *eh*Rad51 homologous DNA pairing

The interaction of mHop2-Mnd1 with *eh*Rad51 and the fact that mHop2-Mnd1 is reported to greatly enhance the D-loop formation catalyzed by human RAD51 [40,57–59], human DMC1 [18,40,60], and *eh*Dmc1 [37] led us to ask if mHop2-Mnd1 would enhance *eh*Rad51-mediated D-loop formation. Using our D-loop formation assay described above (Fig. 5A), we show that inclusion of the mHop2-Mnd1 complex in the reaction greatly stimulated the homologous pairing activity of *eh*Rad51 (33%; Fig. 6B, lanes 2–6). Addition of calcium to the reaction containing mHop2-Mnd1 only provided a slight increase (2–3%) in the amount

of D-loop formed by *eh*Rad51 (Fig. 6B, lanes 8–12). These data suggest *eh*Rad51 D-loop formation is strongly enhanced by mHop2-Mnd1 regardless of the presence of calcium. The ability of murine Hop2-Mnd1 to strongly enhance D-loop formation by the Rad51 recombinase from *E. histolytica* demonstrates that the role of Hop2-Mnd1 in HR is evolutionarily conserved and would suggest that upon availability, *eh*Hop2-Mnd1 would likely enhance the activity of *eh*Rad51.

3.10. mHop2-Mnd1 and calcium stimulate *eh*Rad51 oligonucleotide strand exchange

To shed light on the effect calcium had on *eh*Rad51-mediated recombination, we performed a time course analysis using our oligonucleotide DNA strand exchange assay described above (Fig. 4A). Our results show that DNA strand exchange by *eh*Rad51 is weakly stimulated by the presence of calcium with DNA strand exchange product detected as early as 5 min (Fig. 7A and 7B). The presence of mHop2-Mnd1 resulted in more than a 2-fold stimulation of *eh*Rad51-mediated DNA strand exchange with DNA strand exchange product observed at 5 min (Fig. 7A and 7B). The presence of both calcium and mHop2-Mnd1 provided the greatest enhancement (3-fold) of *eh*Rad51 activity with DNA strand exchange product detectable as early as 2.5 min (Fig. 7A and 7B). These data, along with the D-loop results above, suggest that calcium and mHop2-Mnd1 function in separate but additive ways to promote DNA strand exchange mediated by *eh*Rad51.

3.11. DIDS inhibits *eh*Rad51 strand exchange

Previously, we showed that the commercially available human RAD51 inhibitor DIDS (4,4′-diisothiocyanostilbene-2,2′-disulfonic acid) inhibited *eh*Dmc1 recombinase activities *in vitro* [37]. To determine if DIDS was able to inhibit *eh*Rad51, we performed the oligonucleotide strand exchange assay (Fig. 4A) with increasing concentrations of DIDS. DIDS inhibited *eh*Rad51 DNA strand exchange in a concentration dependent manner (Fig. 8A) with an IC_{50} = 18.5 +/− 2.7 μM. Recently, a small molecule, B02, was reported to inhibit human RAD51 [36]. We wanted to determine if B02 could inhibit *eh*Rad51-mediated DNA strand exchange. Although the strand exchange of human RAD51 is slightly attenuated in the presence of 6% DMSO (Fig. 8B and C, compare lane 2 in both), B02 inhibited the strand exchange activity of human RAD51 (Fig. 8B, lanes 3–5). In contrast, we show that the strand exchange activity of *eh*Rad51 is not affected by the presence of B02 at concentrations that inhibit human RAD51 (Fig. 8B, lanes 7–10). Since we previously reported *eh*Dmc1 was sensitive to inhibition of D-loop formation by DIDS [37], we wanted to investigate whether B02 had an effect on *eh*Dmc1. Similar to *eh*Rad51, B02 had no effect on *eh*Dmc1-mediated DNA strand exchange with concentrations that were able to inhibit human RAD51 (Fig. 8B, lanes 12–15). Importantly, the ability of B02 to inhibit human RAD51 and not *eh*Rad51 or *eh*Dmc1 suggests there may be selectivity among inhibitors of Rad51 between species.

3.12. DIDS disrupts *eh*Rad51 activities through interference with DNA binding

To characterize the effect of DIDS on *eh*Rad51 functions, we first investigated the effect of DIDS on *eh*Rad51 ATP hydrolysis activity. Time course analysis revealed that DIDS stimulated the ATP hydrolysis activity of *eh*Rad51 from 7% to 16% (Fig. 9A), similar to that of human RAD51 [61]. In the presence of dsDNA, there was minimal inhibition (1%) of

*eh*Rad51 in the presence of DIDS. However, DIDS diminished the amount of ATP hydrolyzed by *eh*Rad51 in the presence of ssDNA by 35% (Fig. 9A). This suggested DIDS may be binding to one of the DNA binding sites in *eh*Rad51, which would interfere with the ability of *eh*Rad51 to bind ssDNA or dsDNA. To test this idea, we performed an EMSA to monitor the effect of DIDS on the DNA binding activity of *eh*Rad51. Here, *eh*Rad51 was incubated with ^{32}P-labeled ssDNA or dsDNA in the presence of increasing amounts of DIDS. Our results show that DIDS similarly inhibited ssDNA and dsDNA binding by *eh*Rad51. Specifically, DIDS started to inhibit ssDNA binding at 20 μM (3:1 ratio of DIDS to *eh*Rad51; Fig. 9B, lane 6) and was completely abolished at 40 μM DIDS (6:1 ratio of DIDS to *eh*Rad51; Fig. 9B, lane 8). By comparison, the ability of *eh*Rad51 to bind dsDNA began to be inhibited at 100 μM DIDS (3:1 ratio of DIDS to *eh*Rad51; Fig. 9C, lane 7) and was complete at 150 μM DIDS (4:1 ratio of DIDS to *eh*Rad51; Fig. 9C, lane 7). Interference of *eh*Rad51 ssDNA binding would likely interfere with *eh*Rad51 presynaptic filament dynamics. To test this idea, we used our nuclease protection assay described previously to test the stability of the *eh*Rad51 presynaptic filament in the presence of increasing concentrations of DIDS. Our results show that addition of 30 μM DIDS resulted in complete loss of protection of the ssDNA from DNase I, indicating disruption of *eh*Rad51 presynaptic filament formation (4:1 ratio of DIDS to *eh*Rad51; Fig. 9D, lane 8). This concentration of DIDS is in agreement with the concentration required to disrupt ssDNA binding (Fig. 9B). Together, these data indicate that DIDS interferes with the ability of *eh*Rad51 to bind ssDNA. Our results are in agreement with the mechanism of DIDS inhibition reported for human RAD51 [61] and *eh*Dmc1 [37].

3.13. DIDS inhibits encystation but not proliferation in *E. invadens*

Encystation is thought to involve HR to reduce ploidy [33], and the key enzymes of HR, *eh*Rad51 and *eh*Dmc1 are both expressed during encystation [29]. Because of sensitivity to DIDS *in vitro*, we reasoned that inhibition of the *eh*Rad51 and *eh*Dmc1 recombi-nases with DIDS may disrupt encystation. Unfortunately, induction of encystation in *E. histolytica* has not been reported. Instead, we used the reptilian parasite *Entamoeba invadens* that is often used as a model for studying encystation in *Entamoeba* due to its ability to encyst *in vitro*. To determine the effect of DIDS on encystation of *E. invadens,* cells were induced to encyst in the absence or presence of DIDS (30 μM or 150 μM). In control cells, spherical refractile cysts were readily visualized by light microscopy and, on average, we observed 27.5 +/− 9.7% encystation efficiency in control cells (data not shown) after 48 h in encystation medium. In contrast, very few cysts were observed in DIDS-treated cultures; DIDS significantly inhibited encystation in a dose-dependent fashion (Fig. 10A). To determine the effect of DIDS on the viability of *E. invadens*, cells were induced to encyst in the absence or presence of DIDS (30 or 150 μM) for 48 h, and the viability was measured as a percent of control cells. The final concentrations of control cells (5.6 +/− 3.4 × 10^6 cells/ml) or treated cells (30 μM: 5.3 +/−0.98 × 10^6 cells/ml; 150 μM: 6.7 +/− 3.6 × 10^6 cells/ml) were not significantly different suggesting that the proliferation rate and viability were not hampered by DIDS (Fig. 10B). Therefore, inhibition of encystation was not simply due to cell death.

4. Discussion

The results presented in this report significantly expand on the preliminary findings using partially purified *eh*Rad51 reported by Lopez-Casamichana et al. [29]. Intriguingly we found that many of the biochemical properties of *eh*Rad51 are similar to human RAD51, which is in agreement with the high degree of sequence conservation between the *eh*Rad51 and human RAD51 (66%; Fig. 2 in [42]). For example, in our study, we confirmed that *eh*Rad51 binds ssDNA and dsDNA [29], and our results demonstrate that *eh*Rad51 preferentially bound ssDNA over dsDNA similar to human RAD51 [43]. We show the ATP hydrolysis activity of *eh*Rad51 was enhanced by the presence of dsDNA and ssDNA, with the greatest stimulation occurring in the presence of ssDNA, comparable to human and other Rad51 orthologs [43,44]. Interestingly, the nucleoprotein complexes formed between *eh*Rad51 and ssDNA entered the gel, but failed to form large aggregates that were reported to occur for human RAD51 [43,45]. Nonetheless, these nucleoprotein complexes form stable presynaptic filaments in the presence of ATP and AMP-PNP, providing nearly complete protection of the ssDNA in a nuclease protection assay. Although ADP provided some protection of the ssDNA, the presynaptic filament formed with this nucleotide was not as stable and failed to support DNA strand exchange, like human RAD51 [45]. While it is not clear why some recombinases fail to catalyze strand exchange in the presence of ATP-γ-S, it is possible that the *eh*Rad51 filament that formed in the presence of ATP-γ-S or ADP were partially stable yet nonfunctional or inactive presynaptic filaments. In support of this idea, human RAD51 presynaptic filaments formed in the presence of ATP-γ-S and visualized with electron microscopy, are less extended than an *E. coli* RecA presynaptic filament [53] and resemble the inactive form of *E. coli* RecA filaments found in the absence of a nucleotide cofactor [62]. Studies with human RAD51 and *E. coli* RecA show that the ADP-bound RAD51 or RecA presynaptic filaments are in the inactive conformation, which results in an inability to perform DNA strand exchange [13,63]. Human Dmc1 [48] and *eh*Dmc1 [37] also fail to form D-loop in the presence of ATP-γ-S, whereas human RAD51 was shown to have weak strand exchange activity in the presence of ATP-γ-S [43]. Additionally, in an ATP-dependent manner, *eh*Rad51 effectively facilitated DNA strand exchange over several thousand bases with optimal activity occurring around three nucleotides per *eh*Rad51 monomer as seen with human and yeast Rad51 [44,51,53]. The amount of nicked circular dsDNA formed by *eh*Rad51 (~30%) is similar to that reported for *S. cerevisiae* Rad51 (36%, [44]).

The initial report on *eh*Rad51 by Lopez-Casamichana et al. revealed that partially purified *eh*Rad51 catalyzed D-loop formation [29]. We confirmed these results and show that *eh*Rad51 struggled to catalyze the formation of D-loop even in the presence of calcium, which is known to activate human RAD51 [13]. However, when the HR accessory factor Hop2-Mnd1 was present, *eh*Rad51 was able to efficiently form D-loops. The ability of Hop2-Mnd1 to enhance the homologous DNA pairing and DNA strand exchange activities of human RAD51 [40], *S. pombe* Rad51 [19], and *eh*Rad51 suggests the function of Hop2-Mnd1 is highly conserved. Because calcium adds to the stimulatory effect of Hop2-Mnd1 we suggest that calcium and Hop2-Mnd1 do not overlap in their mechanism of stimulation. Hop2-Mnd1 is reported to promote a conformational change in human RAD51 that

promotes nucleotide and DNA binding [20], and calcium is also proposed to promote a conformational change in the human RAD51 filament [13]. It is possible that mHop2-Mnd1 induces a conformational change in *eh*Rad51 that allows more efficient binding of calcium. Our results demonstrating that mHop2-Mnd1 stimulates the activity of *eh*Rad51, suggest the interaction of Hop2-Mnd1 with Rad51 is evolutionarily conserved. It is reasonable to propose that *eh*Hop2-Mnd1 will likely have a similar effect with *eh*Rad51. Upon availability of purified *eh*Hop2-Mnd1 protein complex, it will be of particular importance to test this hypothesis.

The fact that *eh*Rad51 and *eh*Dmc1 are simultaneously present in *E. histolytica* [29,33,37] suggested the pair of recombinases have complementary activities. Not surprisingly, the DNA binding and ATP hydrolysis activities between *eh*Rad51 and *eh*Dmc1 [37] were similar. Both *eh*Rad51 and *eh*Dmc1 formed stable presynaptic filaments in the presence of ATP and AMP-PNP. Though, the ability to form a presynaptic filament in the presence of ATP-γ-S and ADP was unique to *eh*Rad51. D-loop formation in the absence or presence of calcium was much stronger with *eh*Dmc1 than *eh*Rad51. The plasmid length DNA strand exchange catalyzed by *eh*Rad51 was significantly stronger than reported for *eh*Dmc1 [37]. mHop2-Mnd1 robustly enhanced both *eh*Rad51 and *eh*Dmc1 mediated D-loop formation. Both *eh*Rad51 and *eh*Dmc1 catalyzed oligonucleotide DNA strand exchange, yet we found that *eh*Dmc1 was much more responsive to the presence of calcium, with or without mHop2-Mnd1 present [37]. While these observations are solely from *in vitro* experiments, it is interesting to speculate that *eh*Dmc1 may be involved in early steps of HR that include invasion of the homologous partner and D-loop formation, while *eh*Rad51 may be more adept at later steps such as DNA strand exchange. Taken together, *eh*Rad51 and *eh*Dmc1 may complement each other during HR in *E. histolytica*. Future work will be necessary to test these ideas.

Previously, we demonstrated that DIDS, a small molecule inhibitor of human RAD51 [61], inhibited *eh*Dmc1-mediated activities by disrupting DNA binding [37]. During the course of these studies, the small molecule B02 was reported to be a potent inhibitor of human RAD51 both *in vitro* [36] and *in vivo* [64,65]. We examined the effect of the DIDS and B02 inhibitors on *eh*Rad51 activities. While DIDS inhibited *eh*Rad51 similar to the inhibition we observed with *eh*Dmc1 [37], B02 failed to inhibit either *eh*Rad51 or *eh*Dmc1. The failure of B02 to inhibit either *eh*Rad51 or *eh*Dmc1 is significant because it shows that small molecules such as B02 can discriminate between different Rad51 orthologs. Since our studies showed that DIDS inhibited *eh*Rad51 and *eh*Dmc1-mediated activities [37] *in vitro*, we asked if DIDS would have an effect *in vivo.* While we did not see a decrease in cell viability under the conditions tested, there was a significant decrease in the level of encystation that occurred in the related *E. invadens*. This observation is in agreement with the current idea that HR is important for encystation to occur in *Entamoeba* [33]. Although, DIDS inhibits the activity of *eh*Dmc1 and *eh*Rad51 *in vitro* and decreases the extent of encystation, we are aware that DIDS may be inhibiting encystation through an unknown mechanism that does not depend on the recombinases [66]. In either case, our results demonstrate that small molecules may be tailored to target a specific recombinase, which could be beneficial in identifying potential therapeutics and for studying the role HR plays in the *E. histolytica* life cycle.

The majority of our biochemical understanding of the Rad51 recombinase comes from studies on human and yeast Rad51 proteins. A few biochemical studies on Rad51 from the eukaryotic pathogens *Plasmodium falciparum* [67], *Leishmania infantum* [68], *Ustilago maydis* [69], and *Toxoplasma gondii* [70] reveal that Rad51 from these pathogens possess ATP hydrolysis activity, the ability to bind DNA and/or catalyze D-loop formation. Although the Rad51 recombinases from pathogens have relatively high identity and are closely related to other Rad51 recombinases (Fig. 2 and 3 in [42]), there are differences in their activity. For example, *L. infantum* Rad51 was reported to preferentially bind ssDNA over dsDNA in a manner similar to *eh*Rad51 DNA binding [35]. Contrastingly, the D-loop formation activity of *L. infantum* Rad51 is significantly greater than observed for human RAD51 [68], *S. cerevisiae* Rad51 [14], or *eh*Rad51 in the absence of calcium. While human RAD51 and *eh*Rad51 are both stimulated by the presence of calcium [13], to our knowledge, it is not known whether this is the case for *L. infantum* RAD51 or any other Rad51 from a pathogen. Interestingly, *L. infantum* Rad51, *eh*Rad51 and human RAD51 possess ATP hydrolysis activity in the absence of DNA [35,53]. This is distinct from *S. cerevisiae* and *T. gondii* Rad51 recombinases that possess DNA-dependent ATP hydrolysis activity [44,45,70]. It is possible that these differences observed in the activities of RAD51 from pathogens and human RAD51 may be exploited to develop a potential therapeutic.

HR is important to generate genetic diversity and promote proper chromosome segregation during meiosis. HR also plays a critical role in the repair of DSBs, interstrand cross-links, or DNA adducts in close proximity on opposite strands. DSBs can arise from exogenous sources such as exposure to ionizing radiation and endogenous sources as in the case of a stalled replication fork that occurs due to an attempt to replicate over single-strand break. These stalled replication forks associated with DSBs are reported to be repaired by HR [71–73]. If DSBs are left unrepaired, cell cycle checkpoints are activated potentially leading to cell death [74]. Therefore, it is critical that a DSB is recognized and efficiently repaired. During the life cycle of *Entamoeba,* a uninucleated trophozoite will undergo several rounds of replication to form a tetra-nucleated cyst. The additional rounds of replication increase the probability a stalled or damaged replication fork could occur. Since Rad51 is the key enzyme involved in the search for homology in the sister chromatid, which serves as a template for the repair of the DSB, it is likely to be important to reactivate stalled replication forks [75,76] as *Entamoeba* goes through its life cycle. The relative importance of four nuclei in the cysts of *Entamoeba* species is unknown. Furthermore, genetic exchange among these nuclei has not been reported. However, the presence of transcriptionally active genes that encode the major meiosis-specific genes, including recombinases in *E. histolytica*, [29] supports the idea that such genetic exchange could occur in this stage of the life cycle. Extensive genetic exchange among the nuclei could promote genetic diversity by creating polymorphisms. In support of this possibility, several studies demonstrate that the *E. histolytica* genome possesses extensive polymorphic sequences [77–79]. Indeed, some of these polymorphisms could positively impact fitness in the diverse environments both inside and outside the host. Examples of fitness gains that would benefit the parasite in the host may include acquisition of drug resistance or loss of immune-modulatory antigens. Genetic exchange mediated by *eh*Dmc1 [37] and *eh*Rad51 (current study) is likely to contribute

significantly to the process of generating diverse genomes in multiple life stages of this pathogen.

Acknowledgments

This work was supported in part by the Clemson University Creative Inquiry Program (ER), by Departmental Honors Research Grants from the Calhoun Honors College, Clemson University (AT, ER, and KL), National Science Foundation, DMR-1507266 (SF), Gregg-Graniteville Foundation (SF) and by National Institutes of Health grants R01 GM098510 (MS), R01 CA188347 (AM), R03 AI107950 (LT), R21 AI108287 (LT) and P20GM109094 (LT). The funders had no role in study design, data collection and analysis, decision to publish, or preparation of the manuscript. The authors claim no conflicts of interest. We would like to thank the Sehorn lab and Clark lab for helpful comments on the manuscript. MS and LT conceived and designed the experiments. AK, SG, AS, AT, DS, LL, ER, KL, AVK and CC performed the *in vitro* experiments. SC performed the *in vivo* experiments. AK, SG, SC, LT, and MS analyzed and interpreted the data. AK, SG, SC, AS, and MS contributed to the preparation of the figures. YB, SF, and AM help with the small molecule analysis. AK, SG, LT, and MS wrote the paper.

References

1. San Filippo J, Sung P, Klein H. Mechanism of eukaryotic homologous recombination. Annu Rev Biochem. 2008; 77:229–257. [PubMed: 18275380]
2. Sonoda E, Sasaki MS, Buerstedde JM, Bezzubova O, Shinohara A, Ogawa H, et al. Rad51-deficient vertebrate cells accumulate chromosomal breaks prior to cell death. EMBO J. 1998; 17:598–608. [PubMed: 9430650]
3. Tsuzuki T, Fujii Y, Sakumi K, Tominaga Y, Nakao K, Sekiguchi M, et al. Targeted disruption of the Rad51 gene leads to lethality in embryonic mice. Proc Natl Acad Sci U S A. 1996; 93:6236–6240. [PubMed: 8692798]
4. Cole F, Keeney S, Jasin M. Preaching about the converted: how meiotic gene conversion influences genomic diversity. Ann N Y Acad Sci. 2012; 1267:95–102. [PubMed: 22954222]
5. Symington LS, Rothstein R, Lisby M. Mechanisms and regulation of mitotic recombination in Saccharomyces cerevisiae. Genetics. 2014; 198:795–835. [PubMed: 25381364]
6. Krejci L, Altmannova V, Spirek M, Zhao X. Homologous recombination and its regulation. Nucleic Acids Res. 2012; 40:5795–5818. [PubMed: 22467216]
7. Heyer WD. Biochemistry of eukaryotic homologous recombination. Top Curr Genet. 2007; 17:95–133. [PubMed: 21552479]
8. Sung P, Robberson DL. DNA strand exchange mediated by a RAD51-ssDNA nucleoprotein filament with polarity opposite to that of RecA. Cell. 1995; 82:453–461. [PubMed: 7634335]
9. Bishop DK, Park D, Xu L, Kleckner N. DMC1: a meiosis-specific yeast homolog of E. coli recA required for recombination, synaptonemal complex formation, and cell cycle progression. Cell. 1992; 69:439–456. [PubMed: 1581960]
10. Cloud V, Chan YL, Grubb J, Budke B, Bishop DK. Rad51 is an accessory factor for Dmc1-mediated joint molecule formation during meiosis. Science (New York, NY). 2012; 337:1222–1225.
11. Sugiyama T, Kowalczykowski SC. Rad52 protein associates with replication protein A (RPA)-single-stranded DNA to accelerate Rad51-mediated displacement of RPA and presynaptic complex formation. J Biol Chem. 2002; 277:31663–31672. [PubMed: 12077133]
12. Bugreev DV, Golub EI, Stasiak AZ, Stasiak A, Mazin AV. Activation of human meiosis-specific recombinase Dmc1 by Ca2+ J Biol Chem. 2005; 280:26886–26895. [PubMed: 15917244]
13. Bugreev DV, Mazin AV. Ca2+ activates human homologous recombination protein Rad51 by modulating its ATPase activity. Proc Natl Acad Sci U S A. 2004; 101:9988–9993. [PubMed: 15226506]
14. Chan YL, Brown MS, Qin D, Handa N, Bishop DK. The third exon of the budding yeast meiotic recombination gene HOP2 is required for calcium-dependent and recombinase Dmc1-specific stimulation of homologous strand assimilation. J Biol Chem. 2014; 289:18076–18086. [PubMed: 24798326]

15. Sharma D, Say AF, Ledford LL, Hughes AJ, Sehorn HA, Dwyer DS, et al. Role of the conserved lysine within the Walker A motif of human DMC1. DNA Repair. 2013; 12:53–62. [PubMed: 23182424]
16. Lee MH, Chang YC, Hong EL, Grubb J, Chang CS, Bishop DK, et al. Calcium ion promotes yeast Dmc1 activity via formation of long and fine helical filaments with single-stranded DNA. J Biol Chem. 2005; 280:40980–40984. [PubMed: 16204247]
17. Chi P, San Filippo J, Sehorn MG, Petukhova GV, Sung P. Bipartite stimulatory action of the Hop2-Mnd1 complex on the Rad51 recombinase. Genes Dev. 2007; 21:1747–1757. [PubMed: 17639080]
18. Pezza RJ, Voloshin ON, Volodin AA, Boateng KA, Bellani MA, Mazin AV, et al. The dual role of HOP2 in mammalian meiotic homologous recombination. Nucleic Acids Res. 2014; 42:2346–2357. [PubMed: 24304900]
19. Ploquin M, Petukhova GV, Morneau D, Dery U, Bransi A, Stasiak A, et al. Stimulation of fission yeast and mouse Hop2-Mnd1 of the Dmc1 and Rad51 recombinases. Nucleic Acids Res. 2007; 35:2719–2733. [PubMed: 17426123]
20. Bugreev DV, Huang F, Mazina OM, Pezza RJ, Voloshin ON, Camerini-Otero RD, et al. HOP2-MND1 modulates RAD51 binding to nucleotides and DNA. Nat Commun. 2014; 5:4198. [PubMed: 24943459]
21. Jackson T, Reddy S, Fincham J, Abd-Alla M, Welles S, Ravdin J. A comparison of cross-sectional and longitudinal seroepidemiological assessments of entamoeba-infected populations in South Africa. Arch Med Res. 2000; 31:S36–7. [PubMed: 11070215]
22. Stanley SL Jr. Amoebiasis. Lancet (London England). 2003; 361:1025–1034.
23. Cedeno JR, Krogstad DJ. Susceptibility testing of Entamoeba histolytica. J Infect Dis. 1983; 148:1090–1095. [PubMed: 6140291]
24. Koushik AB, Welter BH, Rock ML, Temesvari LA. A genomewide overexpression screen identifies genes involved in the phosphatidylinositol 3-Kinase pathway in the human protozoan parasite entamoeba histolytica. Eukaryot Cell. 2014; 13:401–411. [PubMed: 24442890]
25. Poxleitner MK, Carpenter ML, Mancuso JJ, Wang CJ, Dawson SC, Cande WZ. Evidence for karyogamy and exchange of genetic material in the binucleate intestinal parasite Giardia intestinalis. Science (New York, NY). 2008; 319:1530–1533.
26. Baez-Camargo M, Gharaibeh R, Riveron AM, de la Cruz Hernandez F, Luna JP, Gariglio P, et al. Gene amplification in Entamoeba histolytica. Invasion Metastasis. 1996; 16:269–279. [PubMed: 9371226]
27. Bhattacharya A, Satish S, Bagchi A, Bhattacharya S. The genome of Entamoeba histolytica. Int J Parasitol. 2000; 30:401–410. [PubMed: 10731563]
28. Mukherjee C, Clark CG, Lohia A. Entamoeba shows reversible variation in ploidy under different growth conditions and between life cycle phases. PLoS Negl Trop Dis. 2008; 2:e281. [PubMed: 18714361]
29. Lopez-Casamichana M, Orozco E, Marchat LA, Lopez-Camarillo C. Transcriptional profile of the homologous recombination machinery and characterization of the EhRAD51 recombinase in response to DNA damage in Entamoeba histolytica. BMC Mol Biol. 2008; 9:35. [PubMed: 18402694]
30. del Charcas-Lopez SM, Garcia-Morales L, Pezet-Valdez M, Lopez-Camarillo C, Zamorano-Carrillo A, Marchat LA. Expression of EhRAD54, EhRAD51, and EhBLM proteins during DNA repair by homologous recombination in Entamoeba histolytica. Parasite (Paris, France). 2014; 21:7.
31. Weber C, Marchat LA, Guillen N, Lopez-Camarillo C. Effects of DNA damage induced by UV irradiation on gene expression in the protozoan parasite Entamoeba histolytica. Mol Biochem Parasitol. 2009; 164:165–169. [PubMed: 19138709]
32. Symington LS. Role of RAD52 epistasis group genes in homologous recombination and double-strand break repair. Microbiol Mol Biol Rev: MMBR. 2002; 66:630–670. (table of contents). [PubMed: 12456786]

33. Singh N, Bhattacharya A, Bhattacharya S. Homologous recombination occurs in Entamoeba and is enhanced during growth stress and stage conversion. PLoS One. 2013; 8:e74465. [PubMed: 24098652]
34. McCulloch R, Barry JD. A role for RAD51 and homologous recombination in Trypanosoma brucei antigenic variation. Genes Dev. 1999; 13:2875–2888. [PubMed: 10557214]
35. McKean PG, Keen JK, Smith DF, Benson FE. Identification and characterisation of a RAD51 gene from Leishmania major. Mol Biochem Parasitol. 2001; 115:209–216. [PubMed: 11420107]
36. Huang F, Motlekar NA, Burgwin CM, Napper AD, Diamond SL, Mazin AV. Identification of specific inhibitors of human RAD51 recombinase using high-throughput screening. ACS Chem Biol. 2011; 6:628–635. [PubMed: 21428443]
37. Kelso AA, Say AF, Sharma D, Ledford LL, Turchick A, Saski CA, DNA, et al. Entamoeba histolytica Dmc1 Catalyzes Homologous, Pairing and strand exchange that is stimulated by calcium and hop2-Mnd1. PLoS One. 2015; 10:e0139399. [PubMed: 26422142]
38. Clark CG, Diamond LS. Methods for cultivation of luminal parasitic protists of clinical importance. Clin Microbiol Rev. 2002; 15:329–341. [PubMed: 12097242]
39. Sanchez LB, Enea V, Eichinger D. Increased levels of polyadenylated histone H2B mRNA accumulate during Entamoeba invadens cyst formation. Mol Biochem Parasitol. 1994; 67:137–146. [PubMed: 7838174]
40. Petukhova GV, Pezza RJ, Vanevski F, Ploquin M, Masson JY, Camerini-Otero RD. The Hop2 and Mnd1 proteins act in concert with Rad51 and Dmc1 in meiotic recombination. Nat Struct Mol Biol. 2005; 12:449–453. [PubMed: 15834424]
41. Sigurdsson S, Trujillo K, Song B, Stratton S, Sung P. Basis for avid homologous DNA strand exchange by human Rad51 and RPA. J Biol Chem. 2001; 276:8798–8806. [PubMed: 11124265]
42. Kelso AA, Goodson SD, Temesvari LA, Sehorn MG. Data on Rad51 amino acid sequences from higher and lower eukaryotic model organisms and parasites. Mol Biochem Parasitol. 2016:d51. (Data in Brief, Submitted).
43. Baumann P, Benson FE, West SC. Human Rad51 protein promotes ATP-dependent homologous pairing and strand transfer reactions in vitro. Cell. 1996; 87:757–766. [PubMed: 8929543]
44. Sung P. Catalysis of ATP-dependent homologous DNA pairing and strand exchange by yeast RAD51 protein. Science (New York, NY). 1994; 265:1241–1243.
45. Chi P, Van Komen S, Sehorn MG, Sigurdsson S, Sung P. Roles of ATP binding and ATP hydrolysis in human Rad51 recombinase function. DNA Repair. 2006; 5:381–391. [PubMed: 16388992]
46. Shalguev VI, Kil YV, Yurchenko LV, Namsaraev EA, Lanzov VA. Rad51 protein from the thermotolerant yeast Pichia angusta as a typical but thermodependent member of the Rad51 family. Eukaryot Cell. 2004; 3:1567–1573. [PubMed: 15590830]
47. Sauvageau S, Stasiak AZ, Banville I, Ploquin M, Stasiak A, Masson JY. Fission yeast rad51 and dmc1, two efficient DNA recombinases forming helical nucleoprotein filaments. Mol Cell Biol. 2005; 25:4377–4387. [PubMed: 15899844]
48. Sehorn MG, Sigurdsson S, Bussen W, Unger VM, Sung P. Human meiotic recombinase Dmc1 promotes ATP-dependent homologous DNA strand exchange. Nature. 2004; 429:433–437. [PubMed: 15164066]
49. Stasiak A, Di Capua E. The helicity of DNA in complexes with recA protein. Nature. 1982; 299:185–186. [PubMed: 7050731]
50. Sheridan SD, Yu X, Roth R, Heuser JE, Sehorn MG, Sung P, et al. A comparative analysis of Dmc1 and Rad51 nucleoprotein filaments. Nucleic Acids Res. 2008; 36:4057–4066. [PubMed: 18535008]
51. Ogawa T, Yu X, Shinohara A, Egelman EH. Similarity of the yeast RAD51 filament to the bacterial RecA filament. Science (New York, NY). 1993; 259:1896–1899.
52. Chow SA, Honigberg SM, Bainton RJ, Radding CM. Patterns of nuclease protection during strand exchange: recA protein forms heteroduplex DNA by binding to strands of the same polarity. J Biol Chem. 1986; 261:6961–6971. [PubMed: 3009481]
53. Benson FE, Stasiak A, West SC. Purification and characterization of the human Rad51 protein, an analogue of E. coli RecA. EMBO J. 1994; 13:5764–5771. [PubMed: 7988572]

54. Sung P, Stratton SA. Yeast Rad51 recombinase mediates polar DNA strand exchange in the absence of ATP hydrolysis. J Biol Chem. 1996; 271:27983–27986. [PubMed: 8910403]
55. Morrison C, Shinohara A, Sonoda E, Yamaguchi-Iwai Y, Takata M, Weichselbaum RR, et al. The essential functions of human Rad51 are independent of ATP hydrolysis. Mol Cell Biol. 1999; 19:6891–6897. [PubMed: 10490626]
56. Logan KM, Knight KL. Mutagenesis of the P-loop motif in the ATP binding site of the RecA protein from Escherichia coli. J Mol Biol. 1993; 232:1048–1059. [PubMed: 8371266]
57. Enomoto R, Kinebuchi T, Sato M, Yagi H, Kurumizaka H, Yokoyama S. Stimulation of DNA strand exchange by the human TBPIP/Hop2-Mnd1 complex. J Biol Chem. 2006; 281:5575–5581. [PubMed: 16407260]
58. Enomoto R, Kinebuchi T, Sato M, Yagi H, Shibata T, Kurumizaka H, et al. Positive role of the mammalian TBPIP/HOP2 protein in DMC1-mediated homologous pairing. J Biol Chem. 2004; 279:35263–35272. [PubMed: 15192114]
59. Pezza RJ, Petukhova GV, Ghirlando R, Camerini-Otero RD. Molecular activities of meiosis-specific proteins Hop2, Mnd1, and the Hop2-Mnd1 complex. J Biol Chem. 2006; 281:18426–18434. [PubMed: 16675459]
60. Pezza RJ, Voloshin ON, Vanevski F, Camerini-Otero RD. Hop2/Mnd1 acts on two critical steps in Dmc1-promoted homologous pairing. Genes Dev. 2007; 21:1758–1766. [PubMed: 17639081]
61. Ishida T, Takizawa Y, Kainuma T, Inoue J, Mikawa T, Shibata T, et al. DIDS, a chemical compound that inhibits RAD51-mediated homologous pairing and strand exchange. Nucleic Acids Res. 2009; 37:3367–3376. [PubMed: 19336413]
62. Yu X, Egelman EH. Structural data suggest that the active and inactive forms of the RecA filament are not simply interconvertible. J Mol Biol. 1992; 227:334–346. [PubMed: 1522597]
63. Stasiak, A.; Egelman, EH. Visualization of recombination reactions. In: Kucherlapati, R.; Smith, GR., editors. Genetic Recombination. American Society for Microbiology; Washington: 1988. p. 265-308.
64. Huang F, Mazin AV. A small molecule inhibitor of human RAD51 potentiates breast cancer cell killing by therapeutic agents in mouse xenografts. PLoS One. 2014; 9:e100993. [PubMed: 24971740]
65. Huang F, Mazina OM, Zentner IJ, Cocklin S, Mazin AV. Inhibition of homologous recombination in human cells by targeting RAD51 recombinase. J Med Chem. 2012; 55:3011–3020. [PubMed: 22380680]
66. Macara IG, Cantley LC. Interactions between transport inhibitors at the anion binding sites of the band 3 dimer. Biochemistry. 1981; 20:5095–5105. [PubMed: 7295667]
67. Gopalakrishnan AM, Kumar N. Opposing roles for two molecular forms of replication protein A in Rad51-Rad54-mediated DNA recombination in Plasmodium falciparum. mBio. 2013; 4:e00252–13. [PubMed: 23631919]
68. Genois MM, Mukherjee A, Ubeda JM, Buisson R, Paquet E, Roy G, et al. Interactions between BRCA2 and RAD51 for promoting homologous recombination in Leishmania infantum. Nucleic Acids Res. 2012; 40:6570–6584. [PubMed: 22505581]
69. Bennett RL, Holloman WK. A RecA homologue in Ustilago maydis that is distinct and evolutionarily distant from Rad51 actively promotes DNA pairing reactions in the absence of auxiliary factors. Biochemistry. 2001; 40:2942–2953. [PubMed: 11258906]
70. Achanta SS, Varunan SM, Bhattacharyya S, Bhattacharyya MK. Characterization of Rad51 from apicomplexan parasite Toxoplasma gondii: an implication for inefficient gene targeting. PLoS One. 2012; 7:e41925. [PubMed: 22860032]
71. Arnaudeau C, Lundin C, Helleday T. DNA double-strand breaks associated with replication forks are predominantly repaired by homologous recombination involving an exchange mechanism in mammalian cells. J Mol Biol. 2001; 307:1235–1245. [PubMed: 11292338]
72. Kim TM, Ko JH, Hu L, Kim SA, Bishop AJ, Vijg J, et al. RAD51 mutants cause replication defects and chromosomal instability. Mol Cell Biol. 2012; 32:3663–3680. [PubMed: 22778135]
73. Schlacher K, Wu H, Jasin M. A distinct replication fork protection pathway connects Fanconi anemia tumor suppressors to RAD51-BRCA1/2. Cancer Cell. 2012; 22:106–116. [PubMed: 22789542]

74. Dasika GK, Lin SC, Zhao S, Sung P, Tomkinson A, Lee EY. DNA damage-induced cell cycle checkpoints and DNA strand break repair in development and tumorigenesis. Oncogene. 1999; 18:7883–7899. [PubMed: 10630641]

75. Cox MM, Goodman MF, Kreuzer KN, Sherratt DJ, Sandler SJ, Marians KJ. The importance of repairing stalled replication forks. Nature. 2000; 404:37–41. [PubMed: 10716434]

76. Michel B, Flores MJ, Viguera E, Grompone G, Seigneur M, Bidnenko V. Rescue of arrested replication forks by homologous recombination. Proc Natl Acad Sci U S A. 2001; 98:8181–8188. [PubMed: 11459951]

77. Haghighi A, Kobayashi S, Takeuchi T, Masuda G, Nozaki T. Remarkable genetic polymorphism among Entamoeba histolytica isolates from a limited geographic area. J Clin Microbiol. 2002; 40:4081–4090. [PubMed: 12409379]

78. Ghosh S, Frisardi M, Ramirez-Avila L, Descoteaux S, Sturm-Ramirez K, Newton-Sanchez OA, et al. Molecular epidemiology of Entamoeba spp.: evidence of a bottleneck (Demographic sweep) and transcontinental spread of diploid parasites. J Clin Microbiol. 2000; 38:3815–3821. [PubMed: 11015408]

79. Zaki M, Clark CG. Isolation and characterization of polymorphic DNA from Entamoeba histolytica. J Clin Microbiol. 2001; 39:897–905. [PubMed: 11230401]

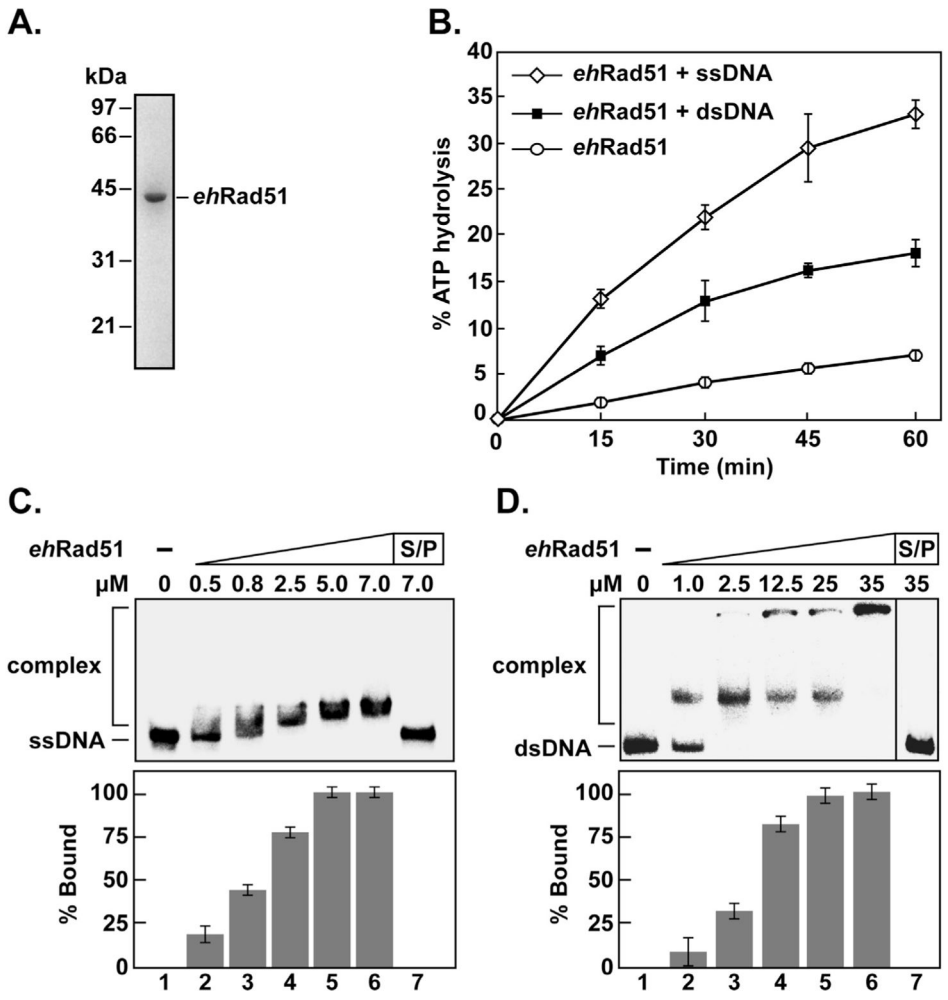

Fig. 1.

*eh*Rad51 hydrolyzes ATP and binds DNA. (A) Purified recombinant *eh*Rad51 (0.5 μg) on a 12% SDS-polyacrylamide gel stained with Coomassie blue. (B) Time course analysis of *eh*Rad51 ATPase activity in the absence and presence of ϕX174 ssDNA or linearized ϕX174 dsDNA. (C) Increasing concentrations of *eh*Rad51 (lanes 2–6) were incubated with ^{32}P-labeled ssDNA, and were resolved on a 12% polyacrylamide gel. (D) Increasing concentrations of *eh*Rad51 (lanes 2–6) were incubated with ^{32}P-labeled dsDNA. The samples were resolved on a 12% polyacrylamide gel. The results for B, C and D were quantified using a phosphorimager and graphed. Lane 1 for C and D contained no protein, and lane 7 for C and D was treated with SDS/PK (S/P). Error bars represent SEM (n = 3).

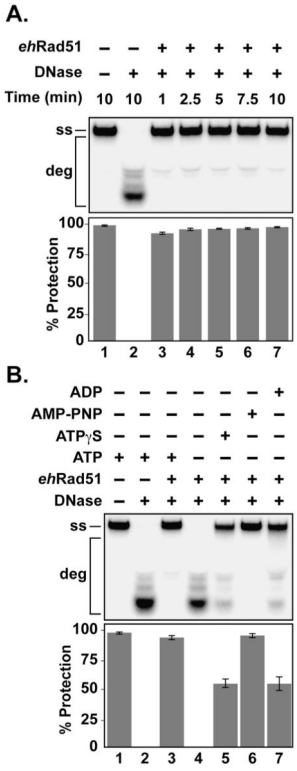

Fig. 2.

*eh*Rad51 forms a nucleoprotein filament. (A) Time course analysis for *eh*Rad51 presynaptic filament formation on ^{32}P-labeled ssDNA (ss) in the presence of DNase I (lanes 3–7). (B) Presynaptic filament formation in the absence and presence of ATP, AMP-PNP, ATP-γ-S, or ADP, as indicated. Samples were resolved on native polyacrylamide gels and analyzed using a phosphorimager. For both (A) and (B), lane 1 contained only ^{32}P-labeled ssDNA, and lane 2 contained ^{32}P-labeled ssDNA and DNase I. The results are from three independent experiments and are presented as percent protection. Error bars represent SEM. Deg, degraded ^{32}P-labeled ssDNA.

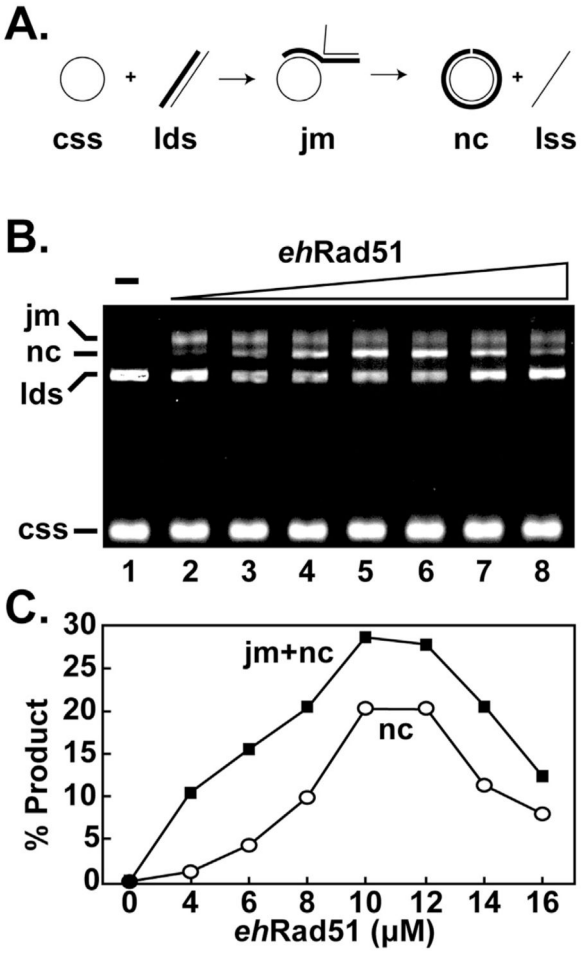

Fig. 3.

*eh*Rad51 facilitates plasmid length homologous DNA pairing and DNA strand exchange. (A) Schematic of plasmid length strand exchange assay. Css, circular ssDNA; lds, linearized dsDNA; jm, joint-molecule; nc, nicked-circular; lss, linearized ssDNA. (B) Increasing concentrations of *eh*Rad51 (lanes 2–8) were incubated with circular ϕX174 ssDNA (css). The reaction was initiated with the introduction of linearized ϕX174 dsDNA (lds) and was deproteinized after 90 min. Reaction products were resolved on an agarose gel and stained with ethidium bromide. Lane 1 contained no protein. (C) The percent product of nicked-circular and total product (jm + nc) were graphed.

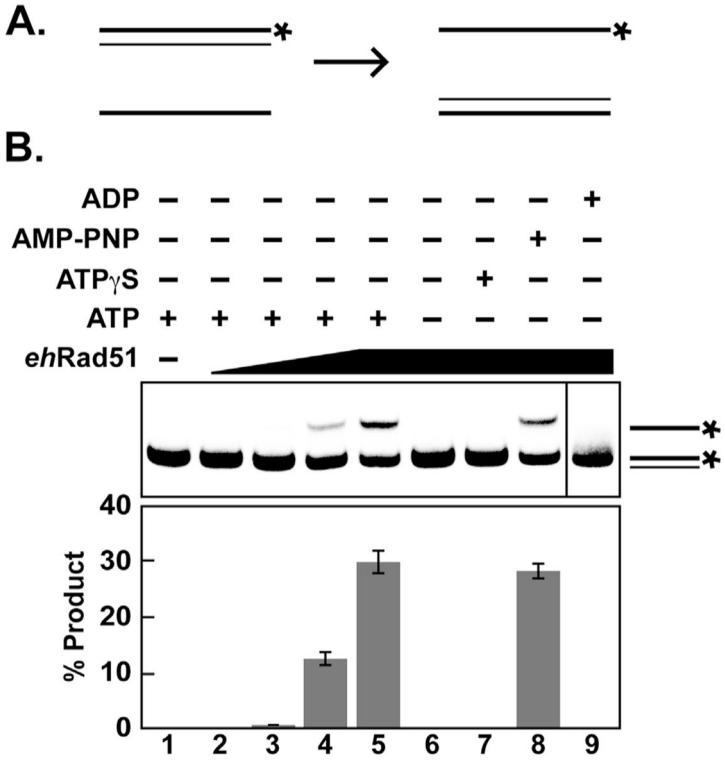

Fig. 4.

*eh*Rad51 mediates oligonucleotide DNA strand exchange. (A) Schematic of oligonucleotide DNA strand exchange assay; * represents ^{32}P-radiolabeled oligonu-cleotide. (B) *eh*Rad51 (0.25 μM, lane 2; 0.5 μM, lane 3; 0.75 μM, lane 4; 1 μM, lanes 5–9) was incubated with unlabeled ssDNA in the presence (lanes 2–5) or absence (lane 6) of ATP, or in the presence of ATP-γ-S (lane 7), AMP-PNP (lane 8), or ADP (lane 9) followed by the addition of radiolabeled dsDNA complex. Lane 1 contained no protein. Reaction products were deproteinized and separated on a 12% non-denaturing polyacrylamide gel followed by analysis of the gels using a phosphorimager. Results from three separate experiments were graphed with DNA strand exchange activity presented as percent product of the displaced ^{32}P-ssDNA. Error bars represent SEM.

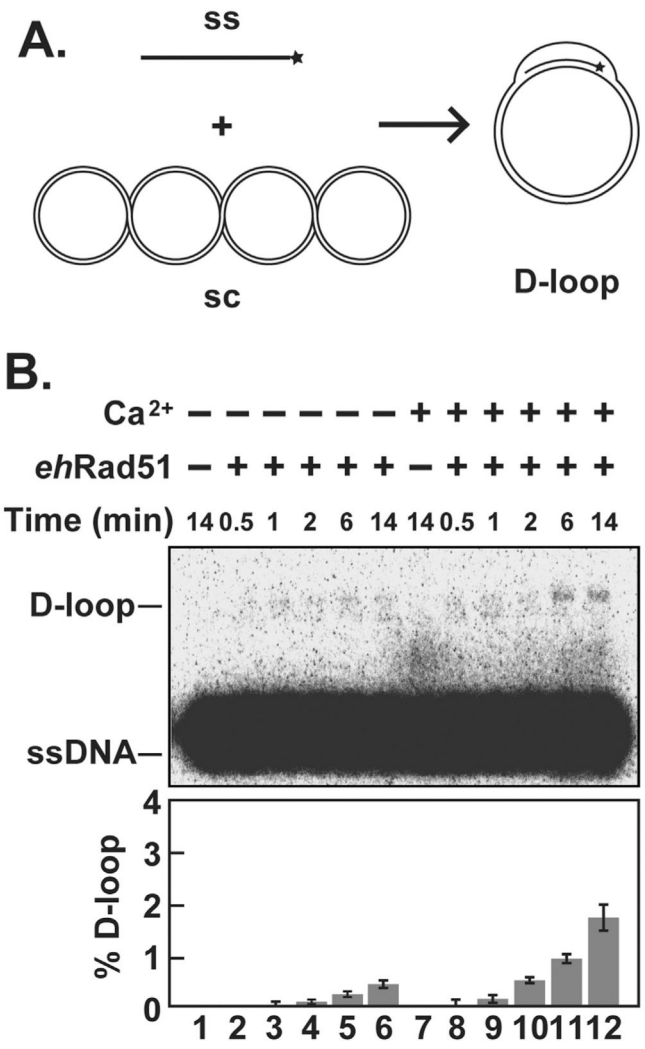

Fig. 5.

Calcium stimulates the homologous DNA pairing activity of *eh*Rad51. (A) Schematic of D-loop formation assay. * represents ^{32}P-radiolabeled oligonucleotide. (B) *eh*Rad51 was incubated with ^{32}P-ssDNA (ss) in the absence (lanes 2–6) or presence of calcium (lanes 8–12). Reactions were initiated by the addition of supercoiled duplex DNA (sc) and were deproteinized at the indicated times. Lane 1 contained no protein, and lane 7 contained calcium and no protein. Reaction products from three independent experiments were analyzed by resolving with agarose gel electrophoresis and quantified using a phosphorimager. Error bars represent SEM.

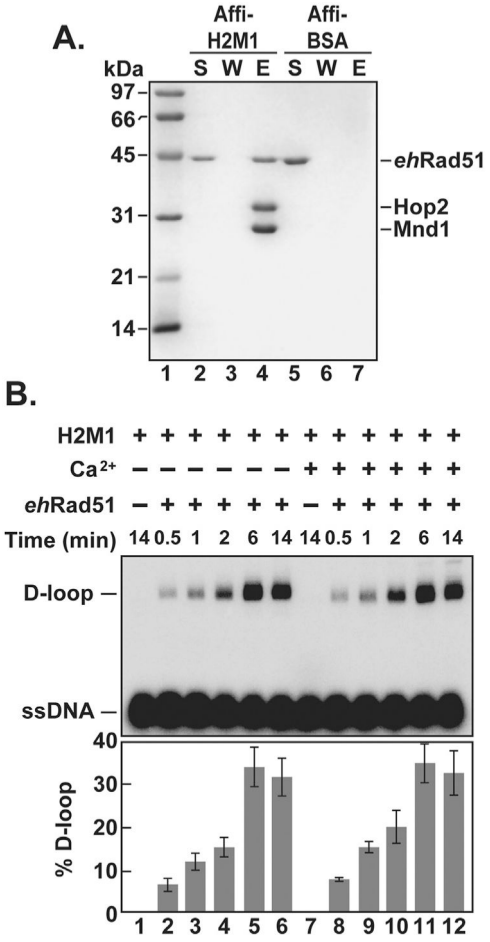

Fig. 6.

mHop2-Mnd1 physically interacts with *eh*Rad51 and enhances *eh*Rad51 homologous DNA pairing activity. (A) *eh*Rad51 was incubated with mHop2-Mnd1 (H2M1) immobilized on Affi-gel or bovine serum albumin (BSA) immobilized on Affi-gel. The supernatant was removed, the beads were washed, and interacting proteins eluted with SDS. Aliquots of the supernatant (S), wash (W), and eluate (E) for Affi-mHop2-Mnd1 (lanes 2–4) and Affi-BSA (lanes 5–7) were separated using 12% SDS-PAGE and stained with Coomassie blue. Lane 1 contained molecular weight markers (sizes indicated). (B) Time course analysis of *eh*Rad51 incubated with ^{32}P-radiolabeled ssDNA for filament formation in the absence (lanes 2–6) or presence (lanes 8–12) of calcium, followed by the addition of mHop2-Mnd1 and supercoiled duplex DNA. Reactions were deproteinized at the indicated times, subjected to agarose gel electrophoresis, and analyzed using a phosphorimager. Lane 1 contained mHop2-Mnd1 and no *eh*Rad51, and lane 7 contained mHop2-Mnd1 and calcium but no *eh*Rad51. Results are represented as percent D-loop formed from three independent experiments. Error bars represent SEM.

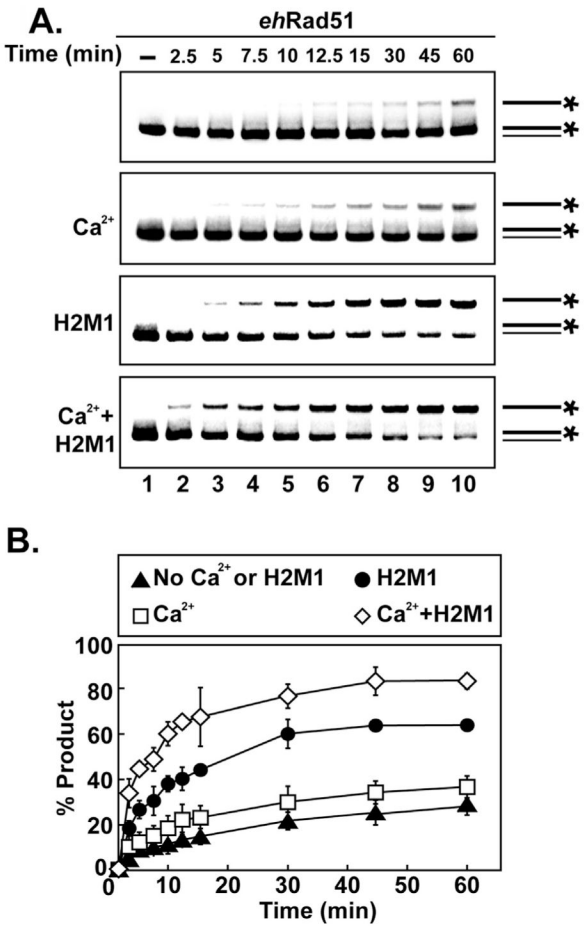

Fig. 7.

*eh*Rad51 oligonucleotide DNA strand exchange activity is stimulated by calcium and mHop2-Mnd1. (A) Time course analysis of *eh*Rad51 in the absence (top row) or presence of calcium (Ca^{2+}, second row), mHop2-Mnd1 (H2M1; third row), or both calcium and mHop2-Mnd1 (Ca^{2+} + H2M1, bottom row). Lane 1 for each condition contained no *eh*Rad51. Reactions were deproteinized at the indicated time points, resolved using native polyacrylamide gel electrophoresis, and analyzed using a phosphorimager. (B) Results from three independent experiments of each condition were quantified and graphed as percent product. Error bars represent SEM.

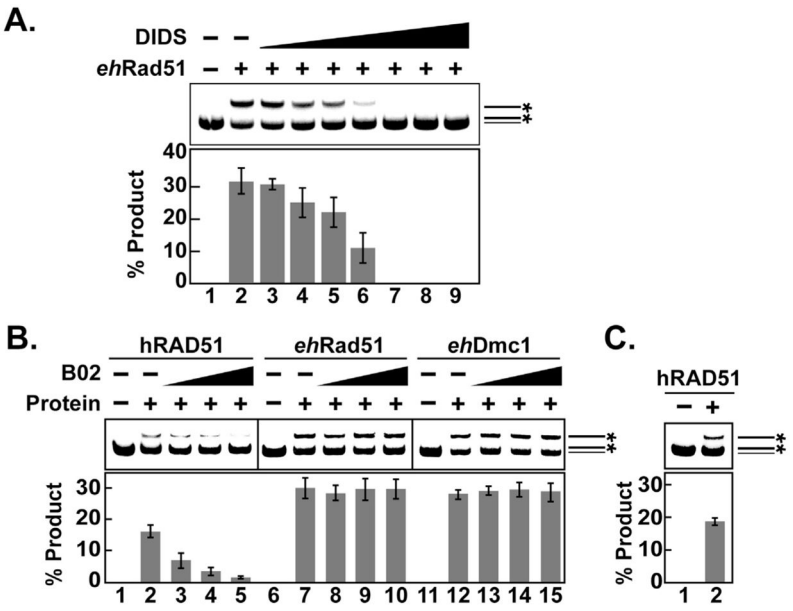

Fig. 8.

*eh*Rad51 DNA strand exchange activity is inhibited by DIDS but not B02. (A) DNA strand exchange analysis of *eh*Rad51 with increasing concentrations of DIDS (2.5, 5, 10, 15, 20, 30, and 40 μM; lanes 3–9, respectively). (B) DNA strand exchange analysis in the presence and absence of increasing concentrations of B02 (100, 200, 300 μM) with human RAD51 (hRAD51; lanes 3–5), *eh*Rad51 (lanes 8–10), and *eh*Dmc1 (lanes 13–15). Each B02 reaction contained 6% DMSO. (C) A control reaction for human RAD51 was performed in the absence of DMSO. The reactions were initiated by the addition ^{32}P-radiolabled duplex DNA. After deproteinization, the reaction products were resolved using non-denaturing PAGE. Lane 1 for A and C and lanes 1, 6, and 11 for B contained no protein. Lane 2 for A and C and lanes 2, 7, and 12 for B were tested in the absence of DIDS or B02 for the indicated recombinase. Percent product formation was graphed, and error bars represent SEM (n = 3).

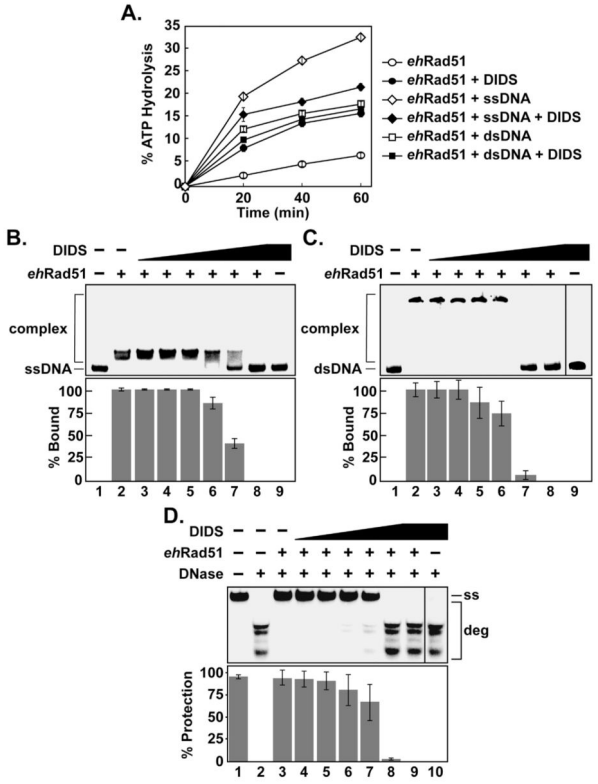

Fig. 9.

DIDS disrupts the DNA binding activity of *eh*Rad51. (A) Time course analysis of *eh*Rad51 ATPase activity in the presence or absence of DIDS (67 μM), with and without ϕX174 ssDNA or linearized ϕX174 dsDNA. Reactions were stopped with the addition of EDTA at the indicated times prior to separation with thin-layer chromatography and phosphorimager analysis. (B) *eh*Rad51 (7 μM) incubated with ^{32}P-radiolabeled ssDNA and increasing amounts of DIDS (5 μM, 10 μM, 15 μM, 20 μM, 30 μM, 40 μM; lanes 3–8 respectively). Lane 1 contained no protein or DIDS. Lane 2 contained no DIDS. Lane 9 contained 40 μM DIDS without *eh*Rad51. (C) *eh*Rad51 (35 μM) incubated with the ^{32}P-radiolabled dsDNA and increasing concentrations of DIDS (20 μM, 40 μM, 80 μM, 100 μM, 150 μM, 200 μM; lanes 3–8 respectively). Lane 1 lacked protein and DIDS, lane 2 contained no DIDS and lane 9 contained 200 μM DIDS and no protein. (D) *eh*Rad51 (7 μM) was incubated with radiolabeled ssDNA in the absence (lane 3) and presence of increasing concentrations of DIDS (5 μM, 10 μM, 15 μM, 20 μM, 30 μM, and 40 μM; lanes 4–9) prior to the addition of DNase I. The reaction were deproteinized, and the products were separated using non-denaturing PAGE. Lane 1 contained radiolabeled ssDNA alone, lane 2 contained DNase with radiolabeled ssDNA, and lane 10 contained radiolabeled ssDNA in the presence of 40 μM DIDS and DNase I. Error bars represent SEM (n = 3).

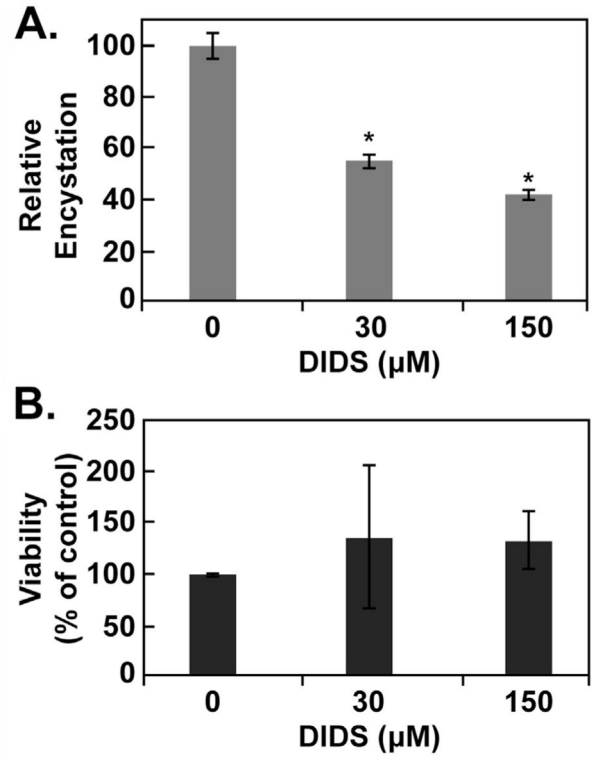

Fig. 10.

DIDS treatment attenuates *E. invadens* encystation but not viability. (A) Cyst formation was scored after 48 h in encystation medium with or without DIDS (**P*<0.05). (B) Cells were incubated with DIDS for 48 h, after which viability was determined. The data from both experiments represent the means ± SD (n = 3).

Table 1

List of oligonucleotide names, sequences, and the assays in which they were used.

Name	Assay	Sequence (5′-3′)
H3	DNA binding	TTGATAAGAGGTCATTTGAATTCATGGCTTAGAGCTT-AATTGCTGAATCTGGTGCTGGGATCCAACATGTTTTAAATATG
H3c	DNA binding	CATATTTAAAACATGTTGGATCCCAGCAC-CAGATTCAGCAATTAAGCTCTAAGCCATGAATTCAAATGACCTCTTATCAA
OL83-1	Strand exchange	AAATGAACATAAAGTAAATAAGTATAAGGATAATACAA-AATAAGTAAATGAAAAACATAGAAAATAAAGTAAAGGATATAAA
OL83-2	Strand exchange	TTTATATCCTTTACTTTATTTTCTATGTTTATTCATTTAC-TTATTTTGTATTATCCTTATACTTATTTACTTTATGTTCATTT
OL90	D-loop/Nuclease protection	AAATCAATCTAAAGTATATATGAGTAAACTTGGTCTGACAGT-TACCAATGCTTAATCAGTGAGGCACCTATCTCAGCGATCTGTCTATTT